

**Theoretical Study on The Electrocatalytic Carbon Dioxide Reduction
over Copper with Copper-based Layered Double Hydroxides**

**Xin-Yu Xu, Jing-Yi Guo, Wei Zhang, Yao Jie, Hui-Ting Song, Hao Lu, Yi-Fan
Zhang, Jia Zhao, Chen-Xu Hu, Hong Yan***

*State Key Laboratory of Chemical Resource Engineering, College of
Chemistry, Beijing University of Chemical Technology, Beijing 100029, China*

Corresponding Author

*(H. Y.) E-mail: yanhong@mail.buct.edu.cn.

ORCID

Hong

Yan:

0000-0003-0285-3704

Contents

Item	Title	Number
Figure	The calculated adsorption energies of COOH on CuAl-Cl-LDHs (001) under the cutoff energies ranging from 260 eV to 450 eV.	S1
	AIMD calculation of (a) CuAl-LDH, (b) Cu@CuAl-LDH, (c) Cu ₂ @CuAl-Cl-LDH, (d) Td-Cu ₄ @CuAl-Cl-LDH and (e) PI-Cu ₄ @CuAl-Cl-LDH in 5000 fs.	S2
	AIMD calculation of extended Cu cluster cell (a) Td-Cu ₄ @CuAl-Cl-LDH and (b) PI-Cu ₄ @CuAl-Cl-LDH in 5000 fs.	S3
	Structural optimization of (a) CuAl-LDH, (b) Cu@CuAl-LDH, (c) Cu ₂ @CuAl-Cl-LDH, (d) Td-Cu ₄ @CuAl-Cl-LDH and (e) PI-Cu ₄ @CuAl-Cl-LDH in the H ₂ O system.	S4
	Standard free energy diagrams for the CO ₂ RR on (a) CuAl-LDH, (b) Cu@CuAl-LDH, (c) Cu ₂ @CuAl-Cl-LDH, (d) Td-Cu ₄ @CuAl-Cl-LDH and (e) PI-Cu ₄ @CuAl-Cl-LDH and the potential energy determines step of five structures above (f).	S5
	Schematic diagram of active site of Cu ₂ @CuAl-Cl-LDH	S6
	Schematic diagram of active site of Td-Cu ₄ @CuAl-Cl-LDH	S7
	Schematic diagram of active site of PI-Cu ₄ @CuAl-Cl-LDH	S8
	Differential charge density map of electrocatalytic CO ₂ reduction intermediates over Td-Cu ₄ @CuAl-Cl-LDH	S9
	Differential charge density map of C-C coupling on CuAl-LDH	S10

	(*CHO→*COCHO)	
	Differential charge density map of C-C coupling on Cu@CuAl-LDH (*CHO→*COCHO)	S11
	Differential charge density map of C-C coupling on Cu ₂ @CuAl-LDH (*COH→*COCOHO)	S12
	Differential charge density map of C-C coupling on Td-Cu ₄ @CuAl-LDH (*CHO→*COCHO)	S13
	Differential charge density map of C-C coupling on PI-Cu ₄ @CuAl-LDH (*COH→*COCOHO)	S14
Table	Formation energy of Cu@CuAl-LDH , Cu ₂ @CuAl-Cl-LDH, Td-Cu ₄ @CuAl-Cl-LDH and PI-Cu ₄ @CuAl-Cl-LDH.	S1
	Screening of Cu ₄ @CuAl-Cl-LDH structural model	S2
	Optimized geometries of electrocatalysis CO ₂ reduction intermediates over two sites on Cu ₂ @CuAl-Cl-LDH and adsorption energy.	S3
	Optimized geometries of electrocatalysis CO ₂ reduction intermediates over two sites on Td-Cu ₄ @CuAl-Cl-LDH and adsorption energy	S4
	Optimized geometries of electrocatalysis CO ₂ reduction intermediates over two sites on PI-Cu ₄ @CuAl-Cl-LDH and adsorption energy.	S5
	The adsorption site of CO ₂ and O-C-O bond angle on the active	S6

site of CuAl-LDH, Cu@CuAl-LDH, Cu₂@CuAl-Cl-LDH, Td-Cu₄@CuAl-Cl-LDH and PI-Cu₄@CuAl-Cl-LDH.

The reaction formula and calculation equation for each S7 elementary step over the surface of the CuAl-LDH, Cu@CuAl-LDH, Cu₂@CuAl-Cl-LDH, Td-Cu₄@CuAl-Cl-LDH and PI-Cu₄@CuAl-Cl-LDH.

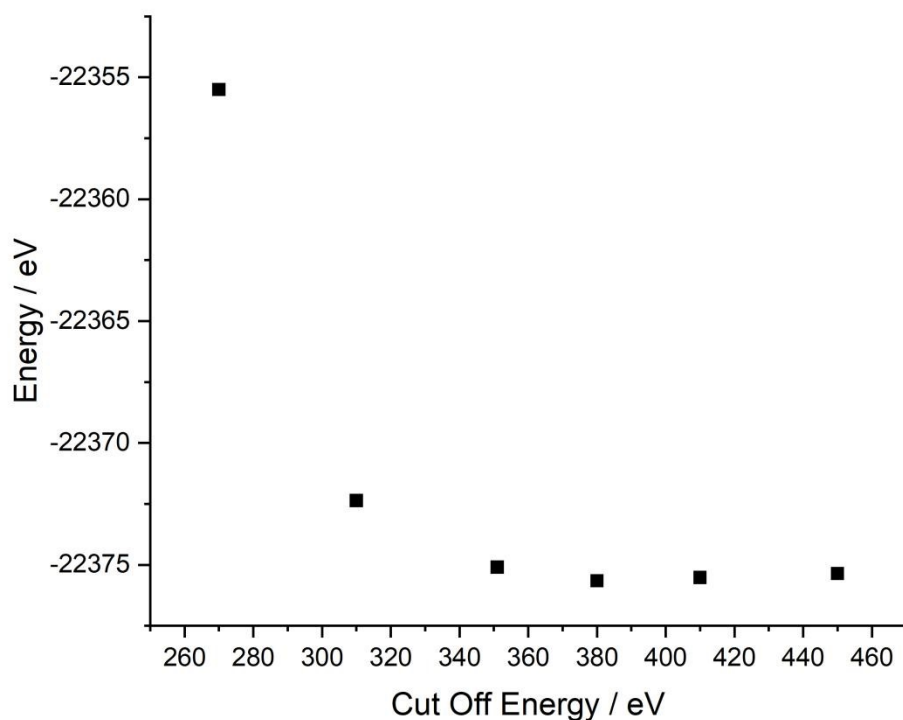


Figure S1. The calculated adsorption energies of COOH on CuAl-Cl-LDHs (001) under the cutoff energies ranging from 260 eV to 450 eV.

As shown in Fig. S1, the energy decreases with increasing cutoff energy, the inflection point is reached at a cutoff energy of 380 eV. Therefore, in this work, the cutoff energy of 380 eV is chosen.

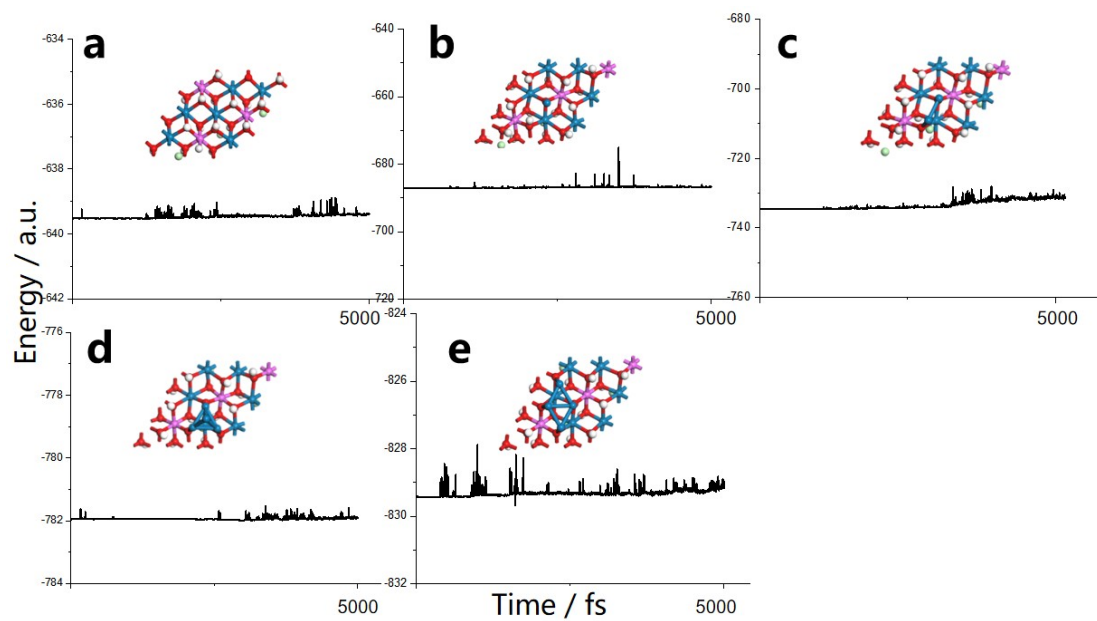


Figure S2. AIMD calculation of (a) CuAl-LDH, (b) Cu@CuAl-LDH, (c) Cu₂@CuAl-LDH, (d) Td-Cu₄@CuAl-LDH and (e) Pl-Cu₄@CuAl-LDH in 5000 fs.

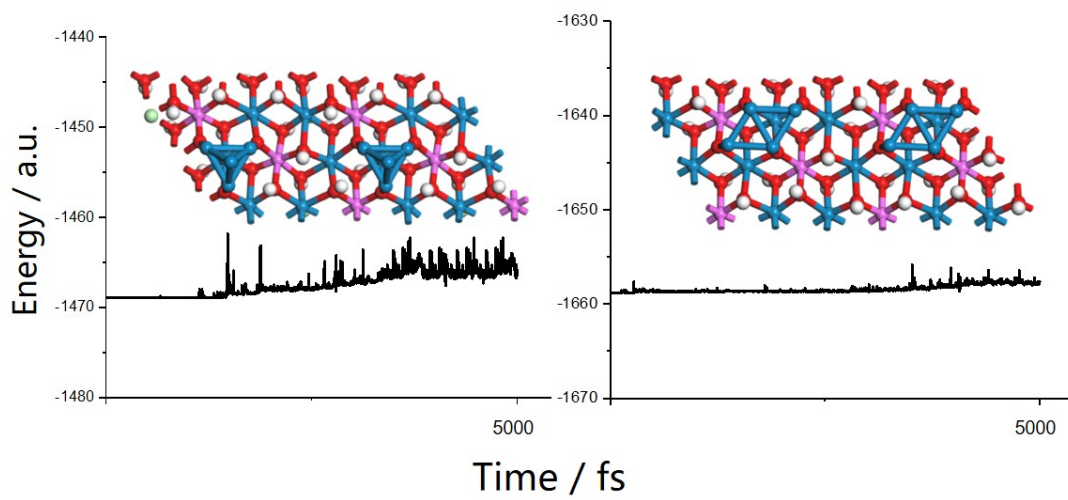


Figure S3. AIMD calculation of extended Cu cluster cell (a) Td-Cu₄@CuAl-Cl-LDH and (b) Pt-Cu₄@CuAl-Cl-LDH in 5000 fs.

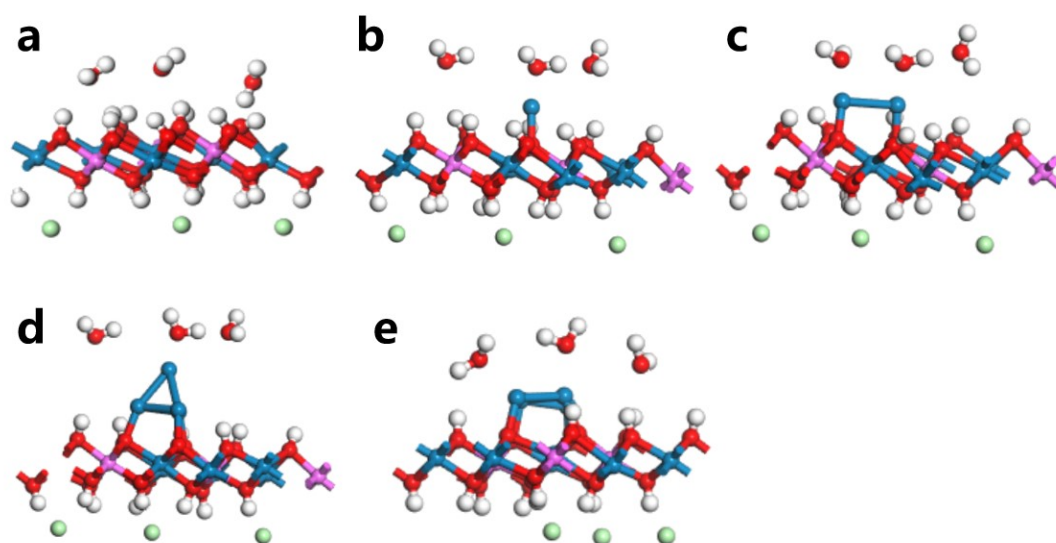


Figure S4. Structural optimization of (a) CuAl-LDH, (b) Cu@CuAl-LDH, (c) Cu₂@CuAl-LDH, (d) Td-Cu₄@CuAl-LDH and (e) Pl-Cu₄@CuAl-LDH in the H₂O system.

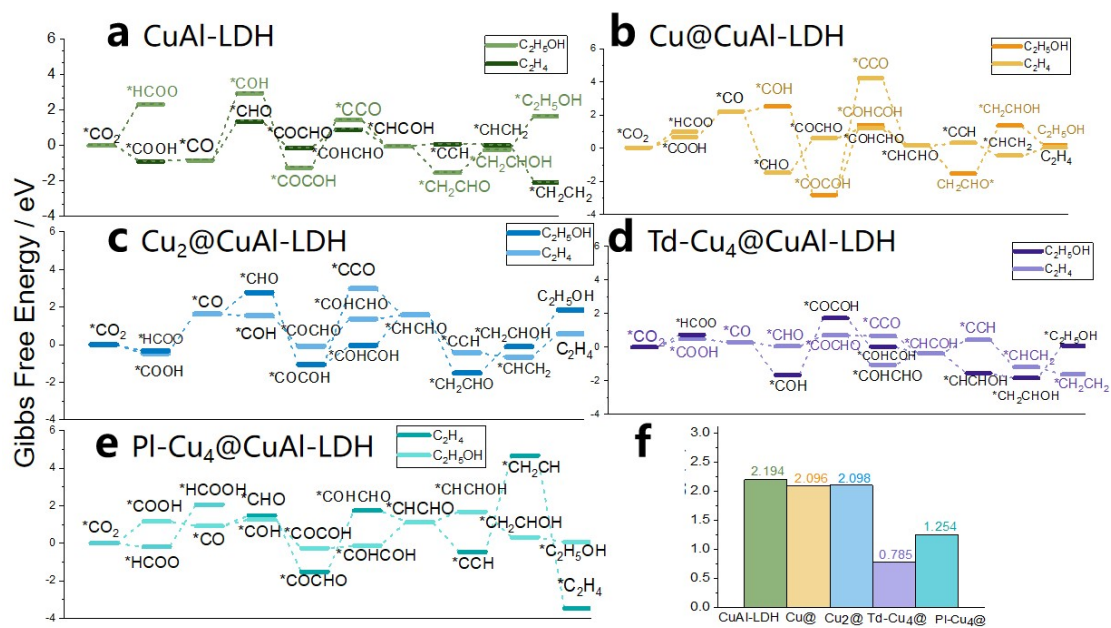


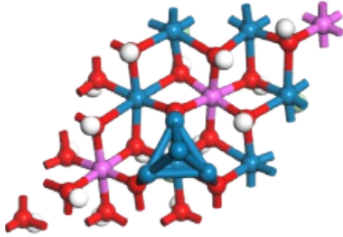
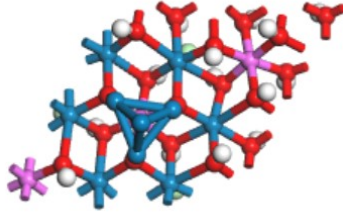
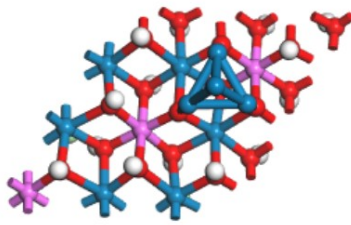
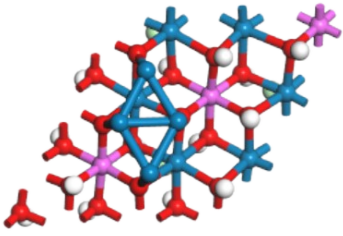
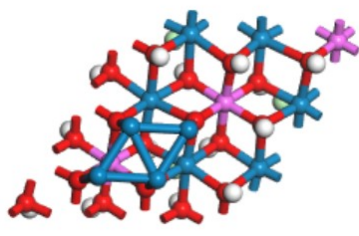
Figure S5. Standard free energy diagrams for the CO₂RR on (a) CuAl-LDH, (b) Cu@CuAl-LDH, (c) Cu₂@CuAl-LDH, (d) Td-Cu₄@CuAl-LDH and (e) PI-Cu₄@CuAl-LDH and the potential energy determines step of five structures above (f).

Table S1. Formation energy of Cu@CuAl-LDH , Cu₂@CuAl-Cl-LDH, Td-Cu₄@CuAl-Cl-LDH and PI-Cu₄@CuAl-Cl-LDH.

	$E_{(\text{LDH}+\text{Cu}_x)}/\text{eV}$	$E_{(\text{LDH})}/\text{eV}$	$E_{(\text{Cu}_x)}/\text{eV}$	$E_{(\text{f})}/\text{eV}$
Cu@CuAl-LDH	-19870.882	-18396.311	-1473.068	-1.503
Cu ₂ @CuAl-LDH	-21329.469	-18379.627	-2948.401	-1.441
Td-Cu ₄ @CuAl-LDH Cu	-24265.547	-18362.044	-5897.611	-5.892
Td-Cu ₄ @CuAl-LDH Al	-24265.450	-18362.468	-5897.611	-5.370
Td-Cu ₄ @CuAl-LDH O	-24264.914	-18362.187	-5897.611	-5.115
PI-Cu ₄ @CuAl-LDH Cu O	-24247.442	-18344.266	-5898.604	-4.572
PI-Cu ₄ @CuAl-LDH Al O	-24247.374	-18344.921	-5898.604	-3.849

Table S2 shows structure of Td-Cu₄@CuAl-Cl-LDH (Cu site) Cu site means orthotetrahedral Cu₄ cluster is at the top of Cu site on CuAl-Cl-LDH PI-Cu₄@CuAl-Cl-LDH (Cu, O sites) which means planar Cu₄ cluster is at the top of Cu site and O site on CuAl-Cl-LDH, the other optimized structures of Cu₄@CuAl-Cl-LDHs (Td-Cu₄@CuAl-Cl-LDH (Al, O site), orthotetrahedral Cu₄ cluster is at the top of Al or O site on CuAl-Cl-LDH PI-Cu₄@CuAl-Cl-LDH (Al, O sites) planar Cu₄ cluster is at the top of Al site and O site on CuAl-Cl-LDH)

Table S2. Screening of Cu₄@CuAl-Cl-LDH structural model.

		$E_{\text{(DFT)}}$ /eV	$E_{\text{(f)}}$ /eV	$E_{\text{(ad)CO}_2}$ / eV
Td-Cu ₄ @CuAl- LDH (Cu site)		-24265.547	-5.892	-1.114
Td-Cu ₄ @CuAl- LDH (Al site)		-24247.604	-5.370	1.302
Td-Cu ₄ @CuAl- LDH (O site)		-24264.914	-5.115	-0.864
Pl-Cu ₄ @CuAl- LDH (Cu, O site)		-24247.442	-4.572	-1.037
Pl-Cu ₄ @CuAl- LDH (Al, O site)		-24247.374	-3.849	-0.531

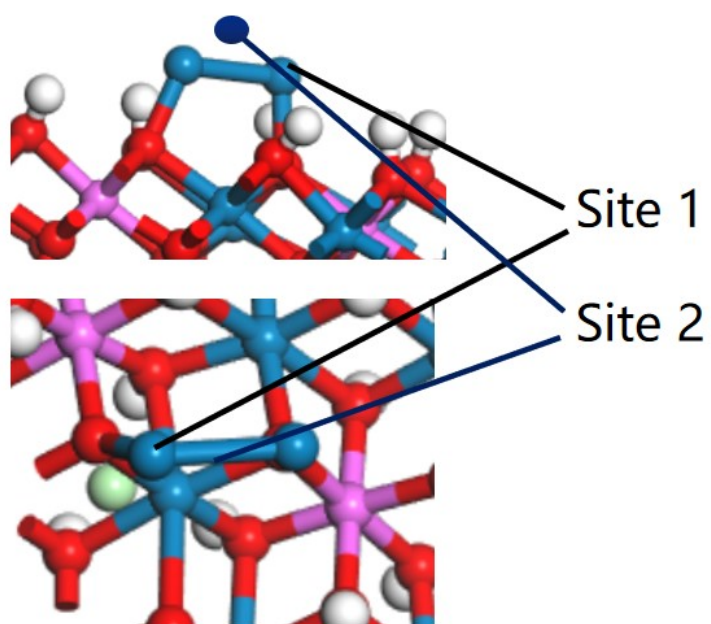
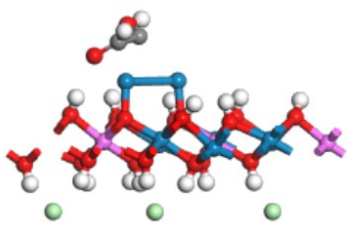
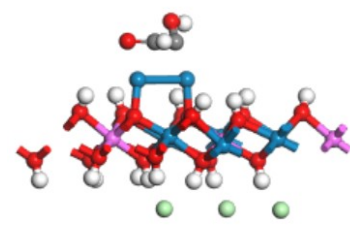
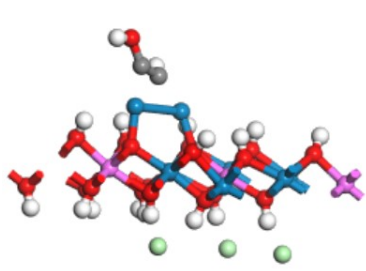
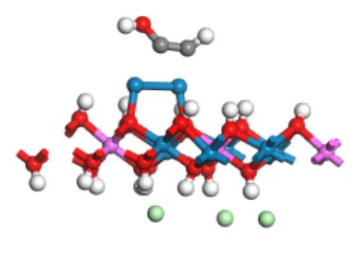
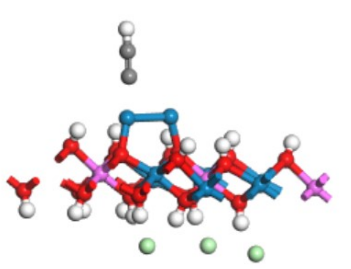
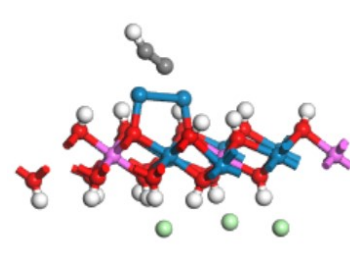
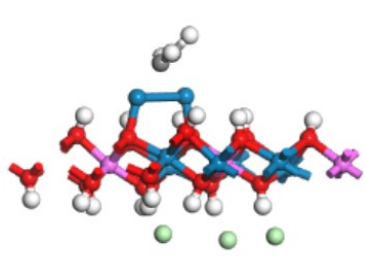
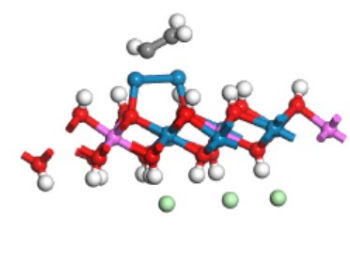
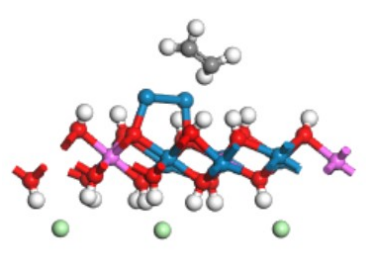
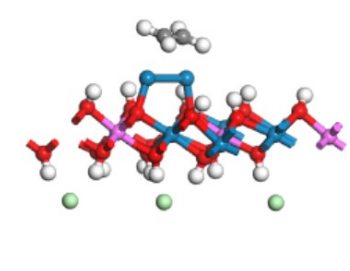


Figure S6. Schematic diagram of active site of Cu₂@CuAl-Cl-LDH.

The top and bottom diagrams represent the side and top views of Cu₂@CuAl-Cl-LDH, respectively, where the blue balls represent copper atoms

Table S3. Optimized geometries of electro catalyzed CO₂ reduction intermediates over two sites (site 1 and site 2) on Cu₂@CuAl-Cl-LDH and adsorption energy.

Site 1	$E_{(ad)}/$ eV	Site 2	$E_{(ad)}/$ eV
*CO ₂	-0.70		-1.73
*COOH	-4.30		-4.75
*CO	-3.22		-3.21
*CHO	-2.46		-3.53
*COCHO	-3.61		-3.44

*COHCH	-3.96		-3.82
O			
*CHCOH	-5.02		-3.37
			
*CCH	-6.80		-6.08
			
*CH ₂ CH	-5.24		-5.12
			
*CH ₂ CH ₂	-2.01		-2.00
			

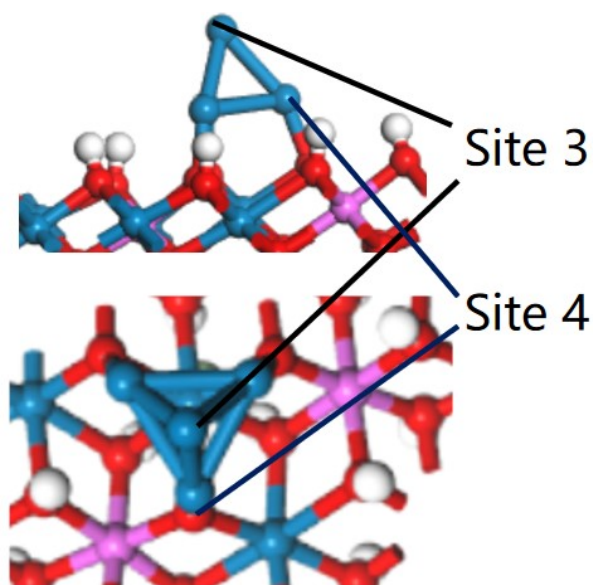
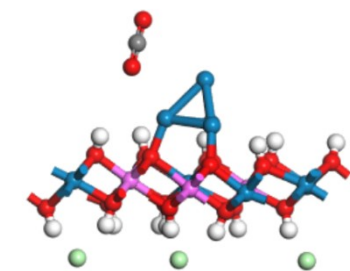
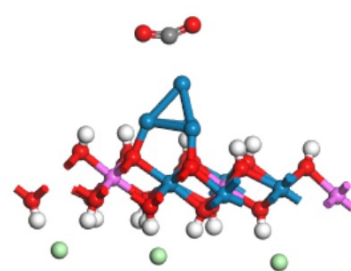
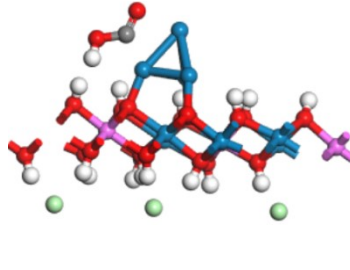
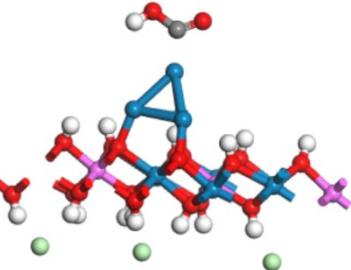
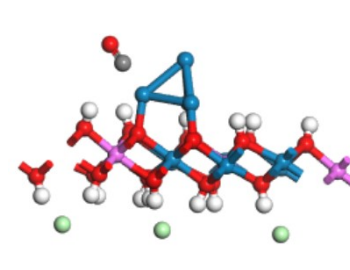
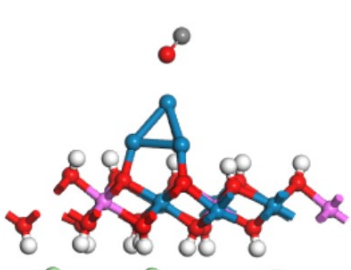
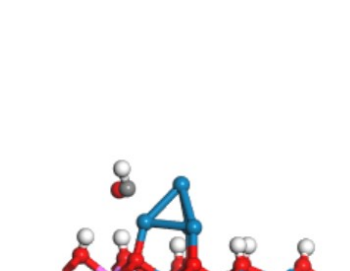
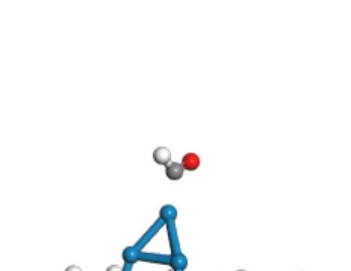


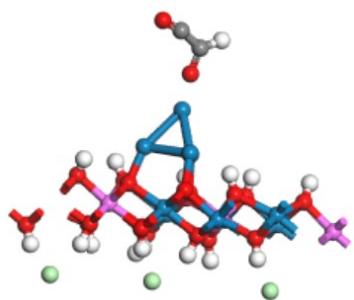
Figure S7. Schematic diagram of active site of Td-Cu₄@CuAl-Cl-LDH.

The top and bottom diagrams represent the side and top views of Td-Cu₄@CuAl-Cl-LDH, respectively, where the blue balls represent copper atoms

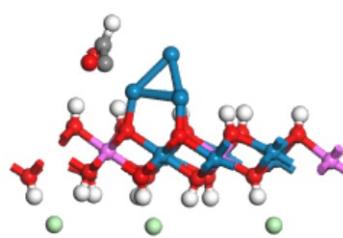
Table S4. Optimized geometries of electro catalyzed CO₂ reduction intermediates over two sites (site 3 and site 4) on Td-Cu₄@CuAl-Cl-LDH and adsorption energy..

Site 3	$E_{(ad)}/$ eV	Site 4	$E_{(ad)}/$ eV
*CO ₂	-1.11		-0.72
			
*COOH	-1.96		-1.53
			
*CO	-1.05		-0.99
			
*CHO	-1.16		-1.38
			

*COCHO

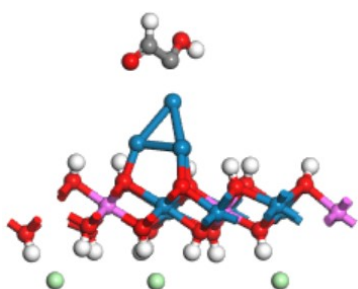


-0.78

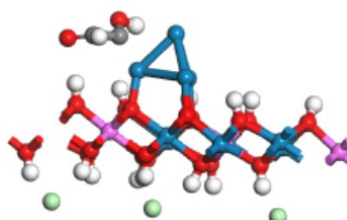


-1.02

*COHCH



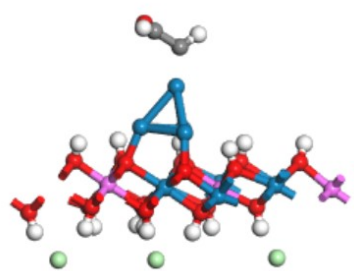
-2.25



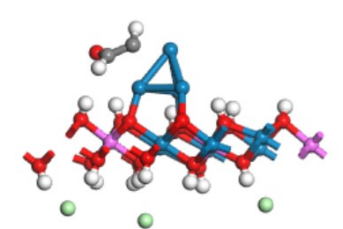
-2.06

O

*CHCHO

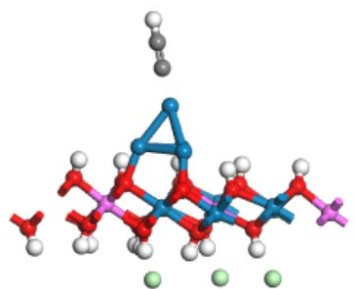


-1.26

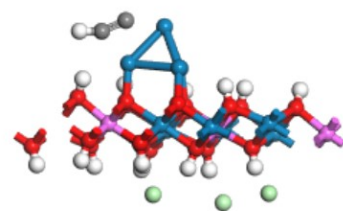


-1.20

*CCH

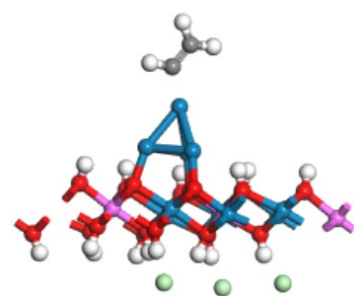


-3.57

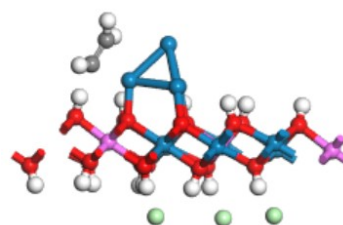


-4.25

*CH₂CH

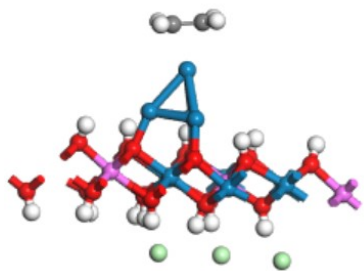


-2.13

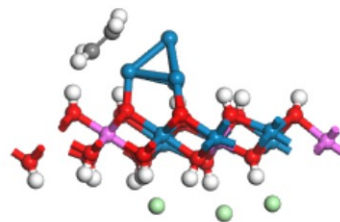


-1.71

*CH₂CH₂



-0.86



-0.61

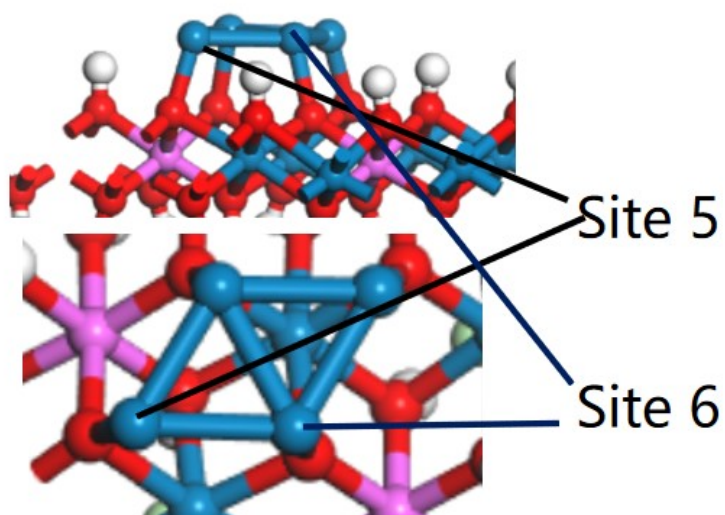
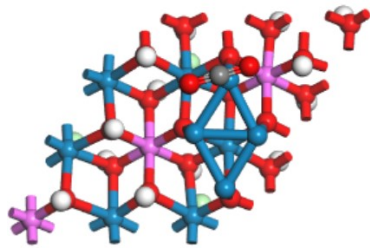
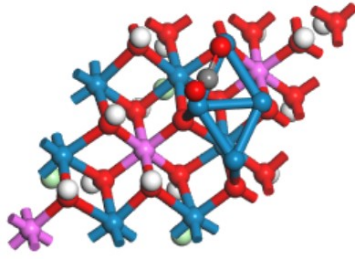
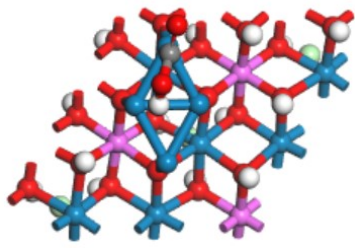
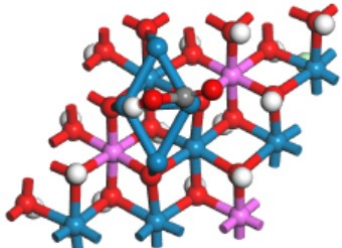
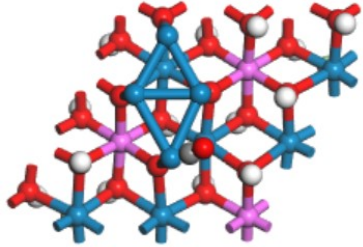
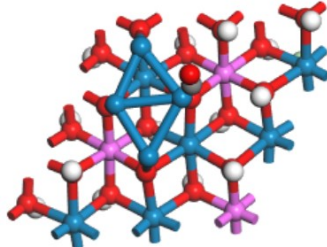
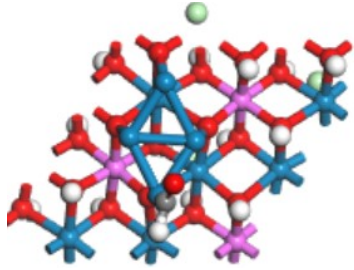
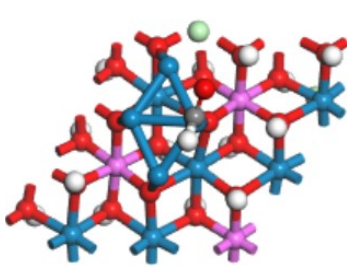
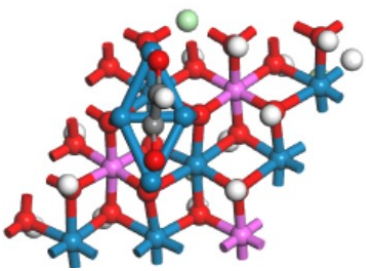
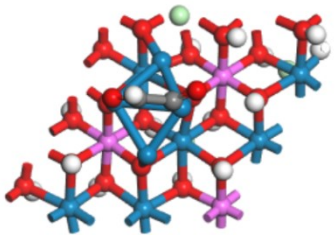
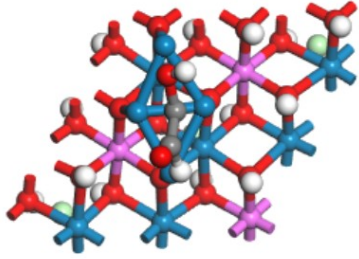
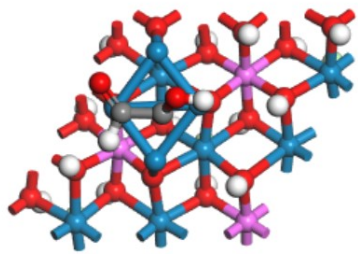
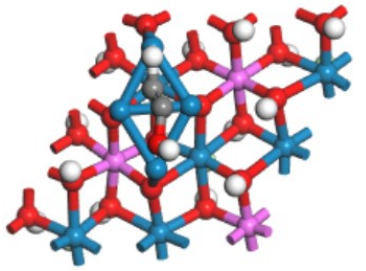
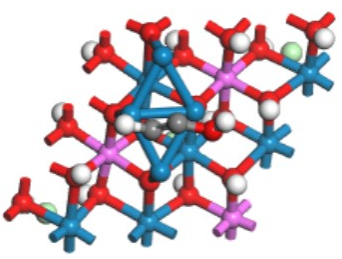
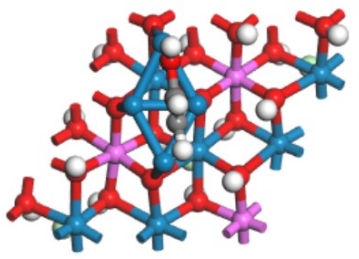
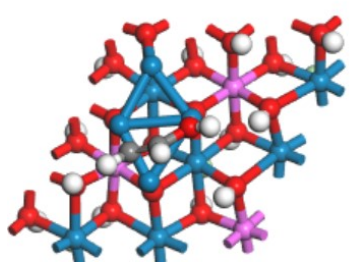
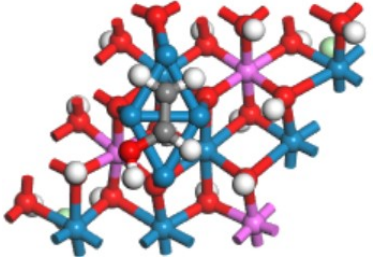
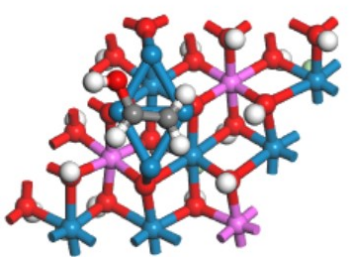
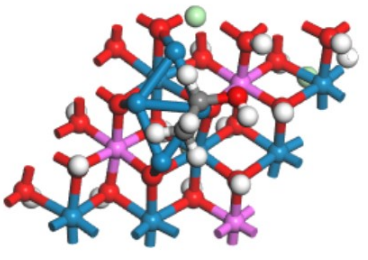
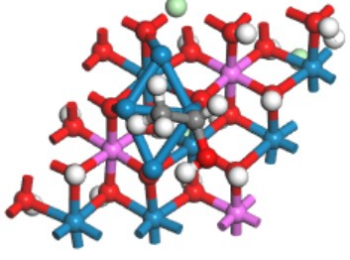


Figure S8 Schematic diagram of active site of PI-Cu₄@CuAl-Cl-LDH.

The top and bottom diagrams represent the side and top views of PI-Cu₄@CuAl-Cl-LDH, respectively, where the blue balls represent copper atoms

Table S5. Optimized geometries of electro catalyzed CO₂ reduction intermediates over two sites (site 5 and site 6) on PI-Cu₄@CuAl-Cl-LDH and adsorption energy.

	Site 5	$E_{(ad)}/$ eV	Site 6	$E_{(ad)}/$ eV
*CO ₂		-1.04		-1.27
*COOH		-3.08		-3.19
*CO		-2.71		-2.41
*CHO		-2.22		-1.99

*COCHO		-4.75		-4.03
*COHCH		-4.43		-6.75
O				
*CHCOH		-5.19		-5.28
*CHCHO		-2.96		-4.27
H				
*CH ₂ CH		-0.43		-0.41
OH				
*C ₂ H ₅ OH		-4.70		-1.27

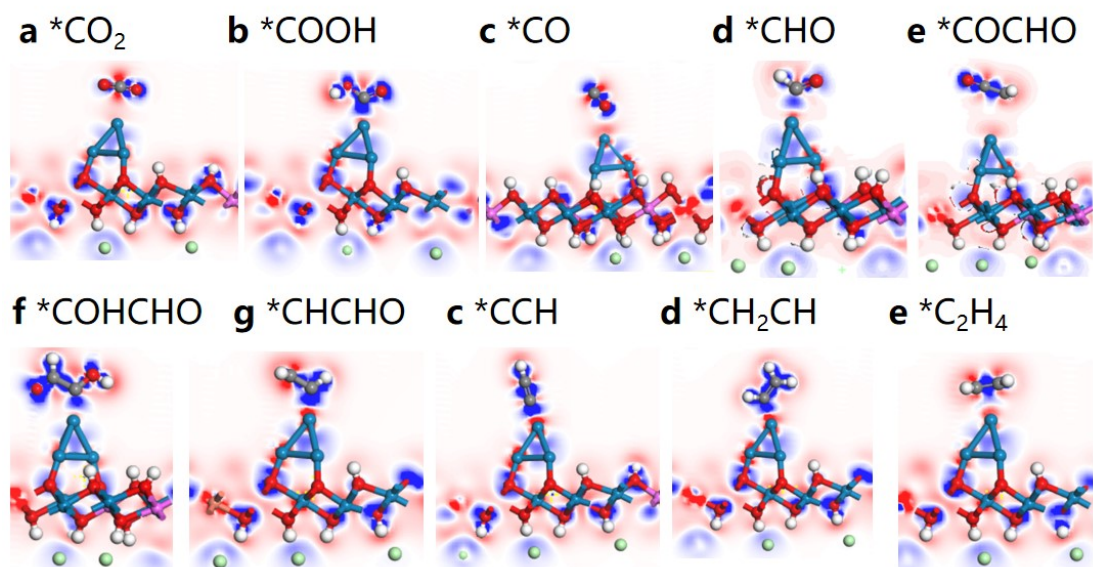
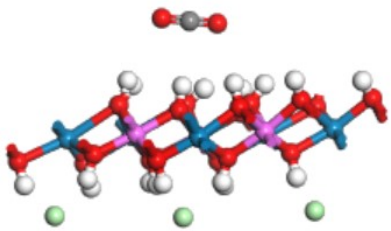
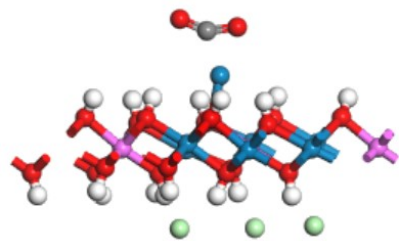


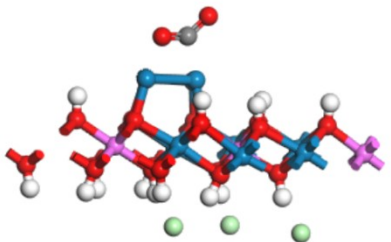


Figure S9. Differential charge density map of electrocatalytic CO₂ reduction intermediates over Td-Cu₄@CuAl-Cl-LDH

Table S6. The adsorption site of CO₂ and O-C-O bond angle on the active site of CuAl-LDH, Cu@CuAl-LDH, Cu₂@CuAl-Cl-LDH, Td-Cu₄@CuAl-Cl-LDH and PI-Cu₄@CuAl-Cl-LDH.

model	∠O-C-O	Adsorption sites
	179.20°	C
	149.05°	C
	161.70°	C
	150.29°	C
	132.98°	C

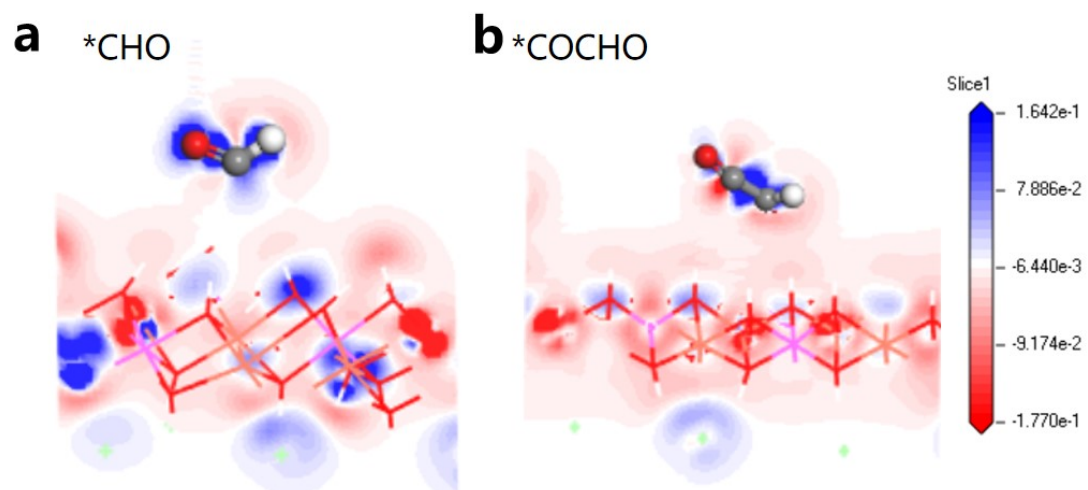


Figure S10. Differential charge density map of C-C coupling on CuAl-LDH

(*CHO→*COCHO)

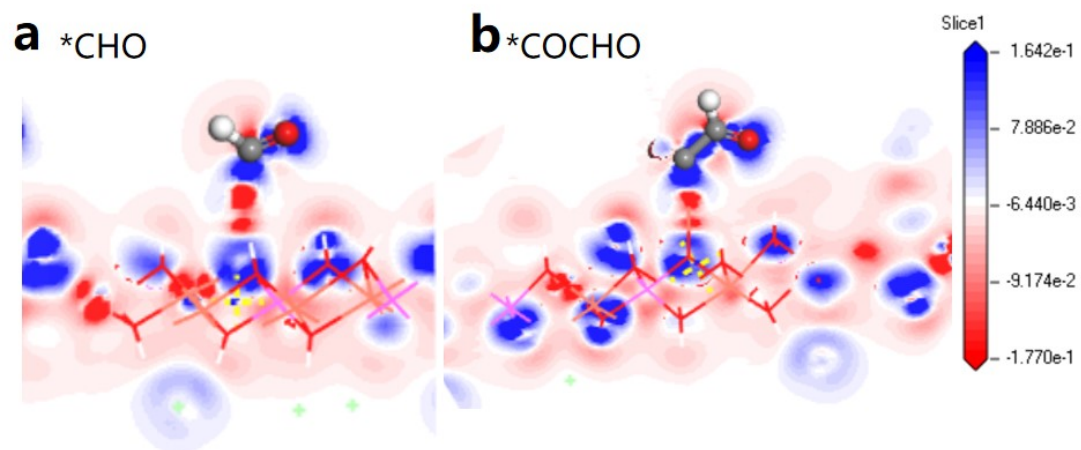


Figure S11. Differential charge density map of C-C coupling on Cu@CuAl-LDH

(*CHO→*COCHO)

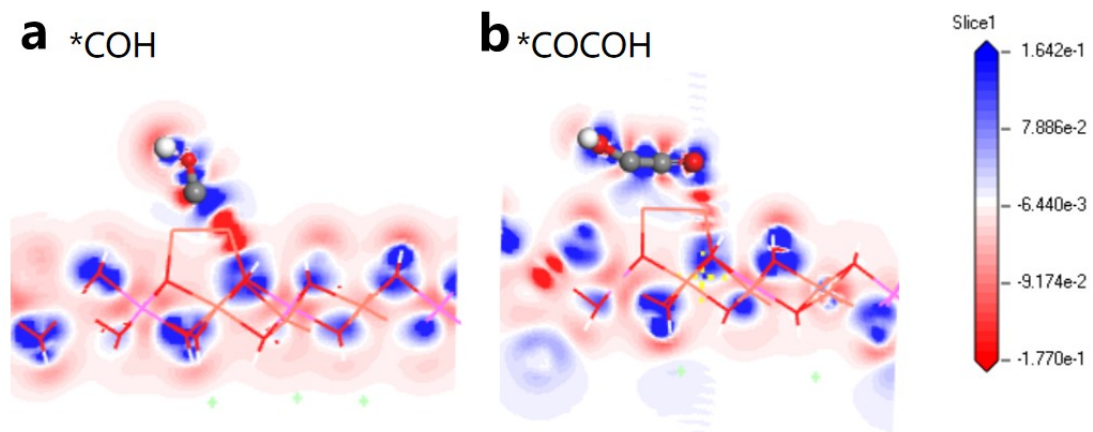


Figure S12. Differential charge density map of C-C coupling on Cu₂@CuAl-LDH

(*COH→*COCOHO)

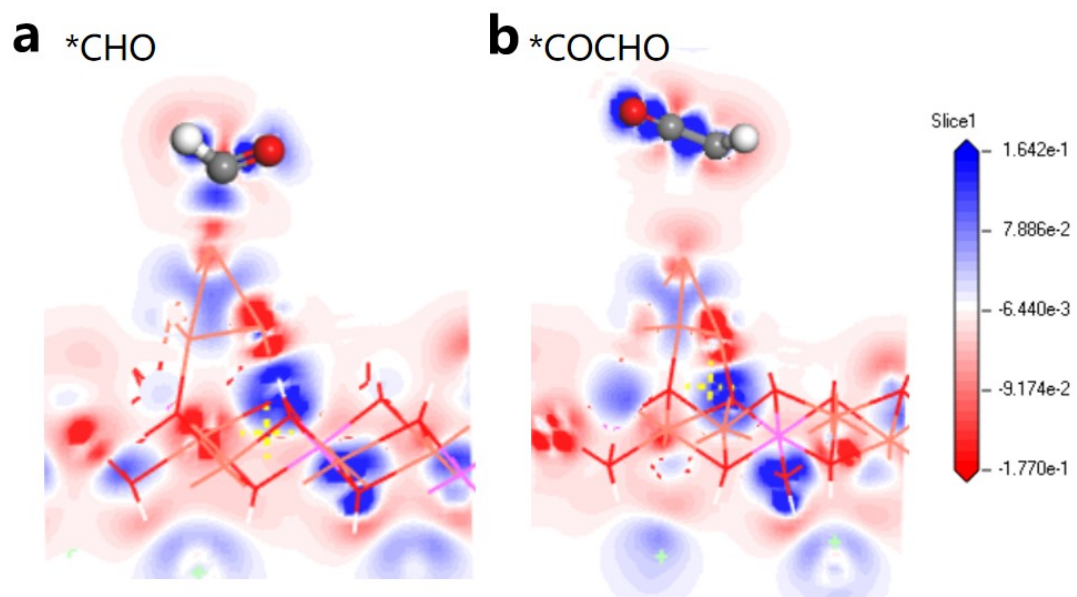


Figure S13. Differential charge density map of C-C coupling on Td-Cu₄@CuAl-LDH

(*CHO → *COCHO)

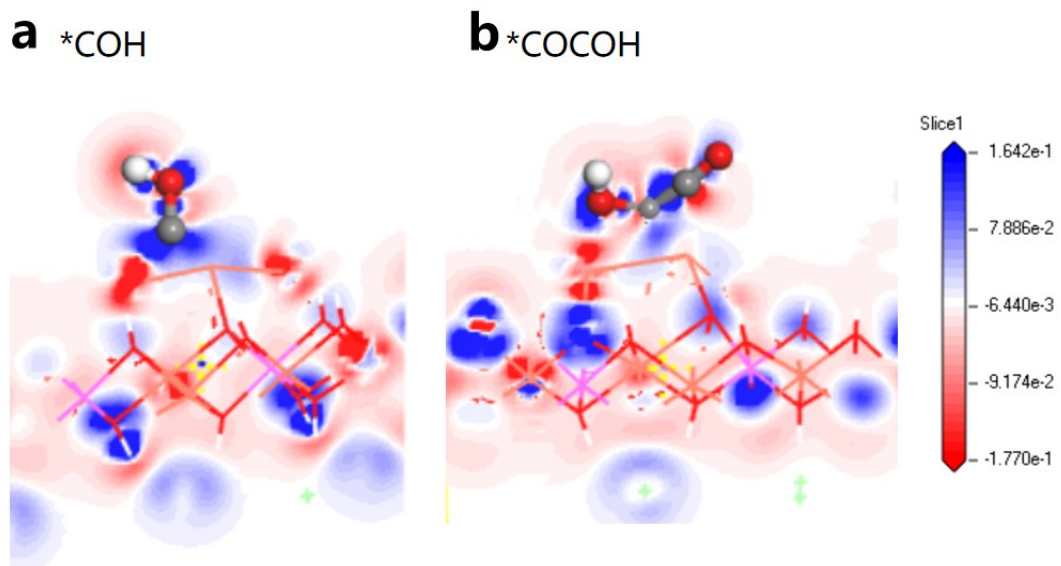


Figure S14. Differential charge density map of C-C coupling on PI-Cu₄@CuAl-LDH

(*COH → *COCOHO)

Table S7. The reaction formula and calculation equation for each elementary step over the surface of the CuAl-LDH, Cu@CuAl-LDH, Cu₂@CuAl-Cl-LDH, Td-Cu₄@CuAl-Cl-LDH and Pl-Cu₄@CuAl-Cl-LDH.

	reaction	equation
R1	$*CO_2+H^++e^- \rightarrow *COOH$	$G_{*COOH}-G_{*CO_2}-0.5G_{H_2}+kT\ln 10 \cdot pH-eU$
R2	$*COOH+H^++e^- \rightarrow *CO$	$G_{*CO}-G_{*COOH}-0.5G_{H_2}+kT\ln 10 \cdot pH-eU$
R3	$*CO+H^++e^- \rightarrow *COH$	$G_{*COH}-G_{*CO}-0.5G_{H_2}+kT\ln 10 \cdot pH-eU$
R4	$*CO+H^++e^- \rightarrow *CHO$	$G_{*CHO}-G_{*CO}-0.5G_{H_2}+kT\ln 10 \cdot pH-eU$
R5	$*COH+*CO \rightarrow *COCOH$	$G_{*COCOH}-G_{*CO}-G_{*COH}+kT\ln 10 \cdot pH-eU$
R6	$*CHO+*CO \rightarrow *COCHO$	$G_{*COCHO}-G_{*CO}-G_{*CHO}+kT\ln 10 \cdot pH-eU$
R7	$*COCOH+H^++e^- \rightarrow *COHCOH$	$G_{*COHCOH}-G_{*COCOH}-0.5G_{H_2}+kT\ln 10 \cdot pH-eU$
R8	$*COCOH+H^++e^- \rightarrow *CCO+H_2O$	$G_{*CCO}+G_{H_2O}-G_{*COCOH}-0.5G_{H_2}+kT\ln 10 \cdot pH-eU$
R9	$*COCHO+H^++e^- \rightarrow *CCO+H_2O$	$G_{*CCO}+G_{H_2O}-G_{*COCHO}-0.5G_{H_2}+kT\ln 10 \cdot pH-eU$
R10	$*COCHO+H^++e^- \rightarrow *CHOCOH$	$G_{*CHOCOH}-G_{*COCHO}-0.5G_{H_2}+kT\ln 10 \cdot pH-eU$
R11	$*COHCOH+2H^++2e^-$ $\rightarrow *CHCOH+H_2O$	$G_{*CHCOH}-G_{*COHCOH}-G_{H_2}+G_{H_2O}+kT\ln 10 \cdot pH-eU$
R12	$*CCO+2H^++2e^- \rightarrow *CHCOH$	$G_{*CHCOH}-G_{*CCO}-G_{H_2}+kT\ln 10 \cdot pH-eU$
R13	$*CCO+2H^++2e^- \rightarrow *CHCHO$	$G_{*CHCHO}-G_{*CCO}-G_{H_2}+kT\ln 10 \cdot pH-eU$
R14	$*CHOCOH+2H^++2e^-$ $\rightarrow *CHCHO+H_2O$	$G_{*CHCHO}-G_{*CHOCOH}-G_{H_2}+G_{H_2O}+kT\ln 10 \cdot pH-eU$

R15	$*\text{CHOCOH} + 2\text{H}^+ + 2\text{e}^-$ $\rightarrow * \text{CHCOH} + \text{H}_2\text{O}$	$G_{*\text{CHCOH}} - G_{*\text{CHOCOH}} - G_{\text{H}_2} + G_{\text{H}_2\text{O}} + kT \ln 10 \cdot \text{pH} - eU$
R16	$*\text{CHCOH} + \text{H}^+ + \text{e}^- \rightarrow * \text{CH}_2\text{COH}$	$G_{*\text{CH}_2\text{COH}} - G_{*\text{CHCOH}} - 0.5G_{\text{H}_2} + kT \ln 10 \cdot \text{pH} - eU$
R17	$*\text{CHCOH} + \text{H}^+ + \text{e}^- \rightarrow * \text{CHCHOH}$	$G_{*\text{CHCHOH}} - G_{*\text{CHCOH}} - 0.5G_{\text{H}_2} + kT \ln 10 \cdot \text{pH} - eU$
R18	$*\text{CHCOH} + \text{H}^+ + \text{e}^- \rightarrow * \text{CCH} + \text{H}_2\text{O}$	$G_{*\text{CCH}} + G_{\text{H}_2\text{O}} - G_{*\text{CHCOH}} - 0.5G_{\text{H}_2} + kT \ln 10 \cdot \text{pH} - eU$
R19	$*\text{CHCHO} + \text{H}^+ + \text{e}^- \rightarrow * \text{CH}_2\text{COH}$	$G_{*\text{CH}_2\text{COH}} - G_{*\text{CHCHO}} - 0.5G_{\text{H}_2} + kT \ln 10 \cdot \text{pH} - eU$
R20	$*\text{CHCHO} + \text{H}^+ + \text{e}^- \rightarrow * \text{CHCHOH}$	$G_{*\text{CHCHOH}} - G_{*\text{CHCHO}} - 0.5G_{\text{H}_2} + kT \ln 10 \cdot \text{pH} - eU$
R21	$*\text{CHCHO} + \text{H}^+ + \text{e}^- \rightarrow * \text{CCH} + \text{H}_2\text{O}$	$G_{*\text{CCH}} + G_{\text{H}_2\text{O}} - G_{*\text{CHCHO}} - 0.5G_{\text{H}_2} + kT \ln 10 \cdot \text{pH} - eU$
R22	$*\text{CH}_2\text{COH} + \text{H}^+ + \text{e}^- \rightarrow * \text{CH}_2\text{CHOH}$	$G_{*\text{CH}_2\text{CHOH}} - G_{*\text{CH}_2\text{COH}} - 0.5G_{\text{H}_2} + kT \ln 10 \cdot \text{pH} - eU$
R23	$*\text{CHCHOH} + \text{H}^+ + \text{e}^- \rightarrow * \text{CH}_2\text{CHOH}$	$G_{*\text{CH}_2\text{CHOH}} - G_{*\text{CHCHOH}} - 0.5G_{\text{H}_2} + kT \ln 10 \cdot \text{pH} - eU$
R24	$*\text{CCH} + 2\text{H}^+ + 2\text{e}^- \rightarrow * \text{CHCH}_2$	$G_{*\text{CHCH}_2} - G_{*\text{CCH}} - G_{\text{H}_2} + kT \ln 10 \cdot \text{pH} - eU$
R25	$*\text{CH}_2\text{CHOH} + 2\text{H}^+ + 2\text{e}^- \rightarrow \text{C}_2\text{H}_5\text{OH}$	$G_{\text{C}_2\text{H}_5\text{OH}} - G_{*\text{CH}_2\text{CHOH}} - G_{\text{H}_2} + kT \ln 10 \cdot \text{pH} - eU$
R26	$*\text{CHCH}_2 + \text{H}^+ + \text{e}^- \rightarrow * \text{CH}_2\text{CH}_2$	$G_{*\text{CH}_2\text{CH}_2} - G_{*\text{CHCH}_2} - 0.5G_{\text{H}_2} + kT \ln 10 \cdot \text{pH} - eU$
R27	$*\text{COH} + * \text{H}^+ + \text{e}^- \rightarrow * \text{CHOH}$	$G_{*\text{CHOH}} - G_{*\text{COH}} - 0.5G_{\text{H}_2} + kT \ln 10 \cdot \text{pH} - eU$
R28	$*\text{CHO} + * \text{H}^+ + \text{e}^- \rightarrow * \text{CHOH}$	$G_{*\text{CHOH}} - G_{*\text{CHO}} - 0.5G_{\text{H}_2} + kT \ln 10 \cdot \text{pH} - eU$
R29	$*\text{COH} + * \text{CO} \rightarrow * \text{COCO H}$	$G_{*\text{COCO H}} - G_{*\text{CO}} - G_{*\text{COH}} + kT \ln 10 \cdot \text{pH} - eU$
